View Article Online / Journal Homepage / Table of Contents for this issue

Performance of multi-configurational calculations for a 1,4-bis(phenylethynyl)benzene derivative conjugated molecule

J. C. Sancho-García* and A. J. Pérez-Jiménez*

Received 10th December 2007, Accepted 5th February 2008
First published as an Advance Article on the web 6th March 2008
DOI: 10.1039/b719080h

Published on 06 March 2008. Downloaded by Michigan State University on 23/01/2016 03:07:12.

The theoretical challenge of finding a single method that quantitatively reproduces both the experimental low-lying excitation energies and the torsional barrier of a prototypical conjugated molecule, which could act as a molecular wire, has been addressed here. The results indicate that this goal can be reasonably achieved when multi-reference perturbation theory up to second order (MRMP2) based on a complete active space self-consistent field (CASSCF) wave function using large active spaces is used. The results obtained were also used to compare with less expensive Kohn–Sham (KS) density functional theory (DFT) calculations when applied to these properties. The results obtained with BLYP and B3LYP exchange–correlation functionals indicate that quantitative agreement with all the experimental data cannot be obtained with this methodology, with a clear dependence on the exchange–correlation form selected. We thus encourage a careful testing of pure and hybrid density functionals whenever KS DFT is used for the rational design of conjugated materials for charge conduits.

1. Introduction

Typically, the simulation of the mode of operation of an organic electronic device (light-emitting diodes, transistors, photo-voltaic cells or molecular wires) requires the accurate description of the main steps related to charge- and energy-transfer processes. Thus, the design of new materials with improved performance needs a fundamental understanding of these processes, which can be in most cases assisted by computational techniques.[1] The performance of these techniques is based on reliable and accurate quantum chemical methods. For instance, the recombination of the charges injected into the electronic levels of the organic material leads to the formation of either singlet or triplet excitons, which can then migrate to finally decay radiatively. Therefore, methodologies based on density functional theory (DFT)[2–4] have continuously grown to become one of the most widespread simulation tools for molecular electronics and photonics, where organic conjugated molecules usually act as building blocks of conducting or light-emitting devices. Although this theory now accompanies the rational study and further design of more efficient systems, its routine application still faces many challenges.[5] Whereas DFT has undoubtedly become very reliable for estimating ground-state properties, the same degree of success has not been encountered when extended to its time-dependent (TD-) version[6–8] to calculate the opto-electronic properties of excited states. In recent systematic studies, the extreme care that must be taken when predicting the opto-electronic properties of conjugated molecules has been thoroughly investigated.[9–15] Since the accuracy of the results strongly depends on the particular form of the exchange–correlation functional chosen,[16,17] a variety of solutions might indeed be found. Hybrid functionals containing a portion of Hartree–Fock (HF)-like exchange usually provide better results[18–26] since some drawbacks of the functionals, self-interaction error and asymptotic behavior of the associated functional derivative among others, are partly improved. The next step is fully orbital-dependent functionals[27–30] which are still far from being widely applied although promising in nature. These features may difficult a solid interpretation of the structure-property guidelines that need to be achieved for further design of novel and more efficient opto-electronic devices. On the other hand, *ab initio* theories are known to be less plagued by these shortcomings of DFT since the exact solution is systematically approached by higher and higher orders of the theory. Moreover, multi-reference versions of these theories,[31,32] despite being far more computationally costly than DFT, have lately experienced important progress since they may be size-consistently applied to excited states as well as to the ground state. Additionally, analytical energy derivatives are also being developed to locate stationary points, which allows their application on the whole potential energy surface. Although those calculations are believed to be barely needed for conjugated materials[33] we show here that they may be the only way to achieve the same good and averaged accuracy for both ground- and excited-state properties.

Rigid rod-shaped conjugated molecules are excellent prototypes for the aforesaid conducting or opto-electronic devices.[34,35] Among them, phenylene ethylene oligomers have been experimentally and theoretically studied for these purposes[36,37] since they could be employed as molecular wires if charged or if experienced an externally applied electric field. The chemical structure of the investigated reference molecule is shown next (the hydrogen atoms of the central core have been omitted for clarity); the molecule is normally terminated

Departamento de Química Física, Universidad de Alicante, E-03080 Alicante, Spain. E-mail: JC.Sancho@ua.es; AJ.Perez@ua.es

 This journal is © the Owner Societies 2008

View Article Online

Published on 06 March 2008. Downloaded by Michigan State University on 23/01/2016 03:07:12.

at both ends by some chemical groups to allow the binding to a substrate:

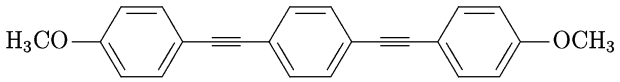

Much has been speculated about the possibility for this and closely related molecules to act as a current-switch[38,39] due to the rotation of the central ring with respect to the side rings under the control of the external voltage. However, recently available experimental results indicate that the barrier height for the rotation of the central arene ring was less than 0.03 eV,[40] suggesting its free rotation at room temperature. The extent to which the theoretical calculations are able to accurately predict the torsional barrier height is thus critical to theoretically corroborate whether the molecule may or may not freely rotate at room temperature between the on (planar) and off (highly twisted) states. These two extreme geometries also differ in their photophysical properties.[41–43] To the best of our knowledge, this is the first high-level multi-configurational study of such a large conjugated molecule; although preliminary studies of the phenylacetylene[44–46] and diphenylacetylene[47] molecules can be found in the literature. These features prompted us to check the validity of state-of-the-art methods to accurately calculate the torsional barrier and low-lying states of this prototypical molecule.

2. Computational methodology

The CASSCF(N,M)-MRMP2 method[48–50] as implemented in the GAMESS package[51] was the main formalism employed; N and M are, respectively, the numbers of electrons and the number of orbitals included in the active space. The calculations consist of two steps. First, an N-in-M wavefunction is determined for each state. This wavefunction is used in the second step as the reference function for the second order perturbation correction.[52] This method, despite the technical difficulties due to the size of the system under study, explicitly includes both non-dynamic and dynamic correlation effects[53] and it properly leads to solutions of multi-configurational nature. Computational strategies to apply these methods efficiently to large systems are being currently pursued.[54–56] Note that analytical gradients are only available for the CASSCF method; thus, the perturbation is actually treated as a single-point correction. The basis sets used (cc-pVDZ: [3s2p1d/2s1p] on first row atoms and hydrogen, respectively, which supposes a number of 480 Cartesian gaussian basis functions) is larger than the smallest recommended basis sets for quantitative applications.[57] The choice of a meaningful active space for the system under study is not a simple issue. Several active spaces of a fully π-character were selected according to the relative energies of the occupied orbitals, and their complementary virtual orbitals, at the restricted Hartree–Fock (RHF) level shown in Table 1: (i) a minimal space (2,2) based on a reduced HOMO (highest occupied molecular orbital) and LUMO (lowest unoccupied molecular orbital) occupation; (ii) a nearly minimal active space (4,4) built by adding the (H-1)OMO and (L + 1)UMO orbitals to the previous space; and (iii) the largest possible formed by all the energetically close active valence π-orbitals, the (12,12) active space. Table 1 also shows that extending the π-based active space would need to consider a (16,16) window. However, the next B_u and A_g orbitals cannot be strictly considered part of the π-space since they represent combinations of the p orbitals of the ethylenic groups and thus lying in the plane of symmetry of the molecule. For this reason we limit ourselves to the (12,12) active space. We show the relevant molecular orbitals in Fig. 1. On the other hand, active spaces as large as (16,16) are beyond the current computational capabilities of most codes for such number of orbitals. Correlation contributions involving the valence and inactive orbitals of the multi-reference wavefunction are then treated at the perturbative level. The symmetry of the molecule was always fixed at the C_{2h} point group, which implies the ^1A_g, ^1B_u, and ^3B_u electronic states for the ground and first excited states of each singlet and triplet symmetry, respectively.

The results from the *ab initio* calculations were compared with those from DFT since this method is nowadays one of the most widespread simulation tools. The high accuracy of DFT methods in predicting ground-state properties has encouraged the direct application of exchange–correlation functionals to excited-state properties within a time-dependent response framework (TD-DFT). The well-known BLYP[58,59] and B3LYP[60,61] exchange–correlation functionals were selected; the latter includes a fraction (20%) of HF-like exchange, but calculated with the Kohn–Sham orbitals, which has been shown to be crucial for accurate calculations of the same nature than those performed here. Note that DFT may be adiabatically applied to the lowest state of each symmetry (S_0 and T_1 here);[62] vertical transitions energies at the optimized DFT geometry for the ground-state were however calculated at the TD-DFT level. These calculations were done with the Gaussian03 package[63] using the default yet accurate integration grid.[64]

3. Results and discussion

3.1 Optimized geometries of ground and excited states

Since the geometry of the excited states has been fully relaxed at the CASSCF(12,12) level, we have analyzed the way the geometry of the molecule is modified upon photoexcitation. To do so, we consider as the most relevant parameter the evolution of the bond-length alternation (BLA) along the backbone; it is defined at site i as the difference between the lengths of the (i, i + 1) and (i, i − 1) O–C or C–C bonds. Note

Table 1 Details of the RHF orbitals employed to select the active spaces and their relative energy (in eV) with respect to the HOMO level

Ordering	(H-8)OMO	(H-7)OMO	(H-6)OMO	(H-5)OMO	(H-4)OMO	(H-3)OMO	(H-2)OMO	(H-1)OMO	HOMO
Label	A_u	A_g	B_u	B_g	A_u	B_g	B_g	A_u	B_g
Energy	−3.8	−3.4	−3.3	−2.3	−2.3	−2.2	−2.2	−1.0	0.0

View Article Online

Published on 06 March 2008. Downloaded by Michigan State University on 23/01/2016 03:07:12.

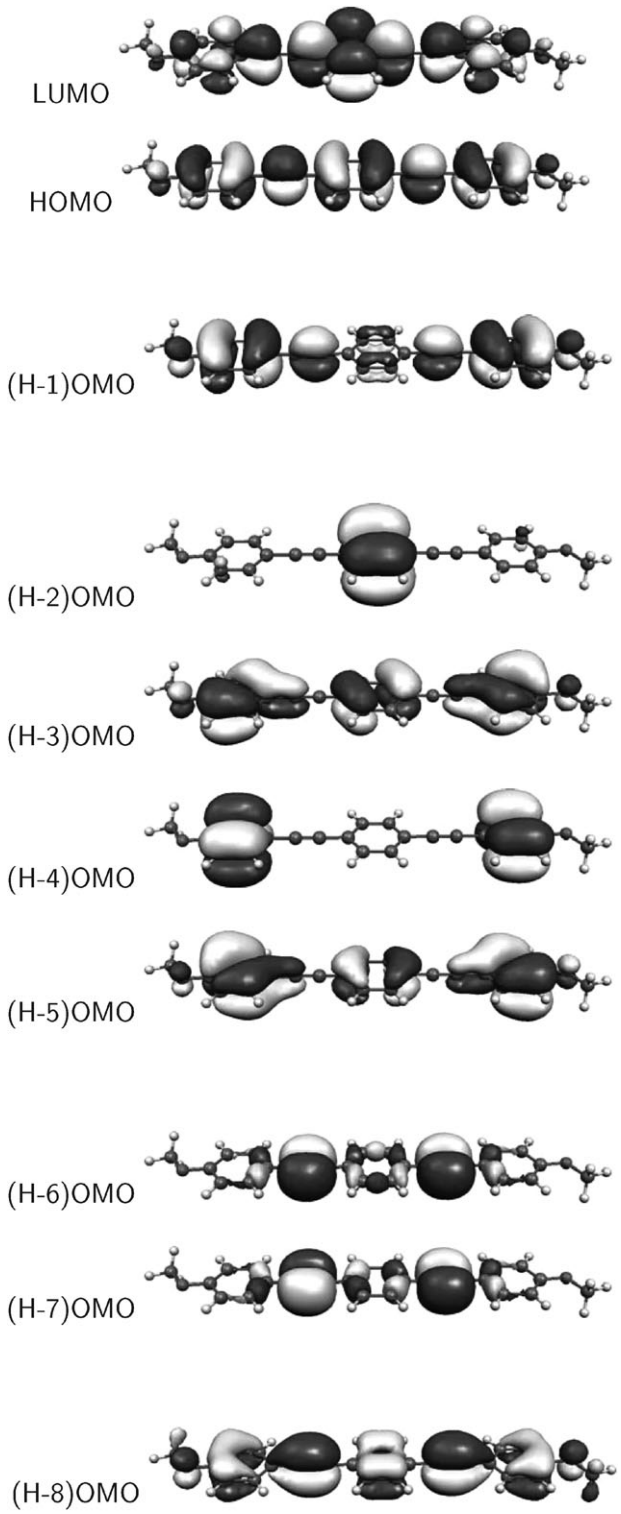

Fig. 1 Contour plots (from top to bottom) of the lowest unoccupied molecular orbital and highest occupied molecular orbitals (see Table 1 for their symmetry label and relative energy) at the RHF ground state optimized geometry.

that the numbering starts from the first non-hydrogen atom (see Fig. 2). The extent of the changes in bond lengths serves as a measure for the localization of the excited state; significant changes are involved in the accommodation of the new

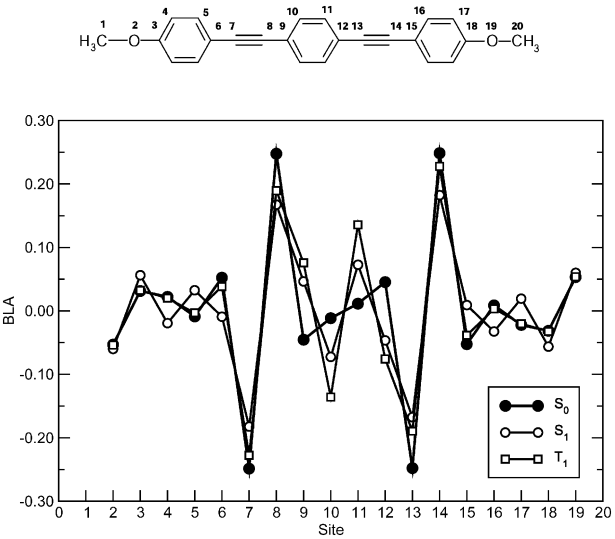

Fig. 2 Evolution with site position *i* of the BLA (in Å) as calculated at the CASSCF(12,12) level (see chemical structure on top for site labels).

electronic configuration. Fig. 2 displays the BLA for the three states considered. The BLA pattern in the ground state clearly shows the aromaticity of the benzene rings and the presence of the acetylenic bond, whose distance (1.1958 Å) is calculated to be very similar to that of a normal C–C triple bond. Going to the first singlet excited state we found the following features with respect to the ground state: (i) all the benzene rings are characterized now by a more pronounced quinoid structure; and (ii) the acetylenic bond is much longer (1.2200 Å) while the linkage bonds are much shorter by 0.04–0.06 Å. These changes occur symmetrically around the central benzene ring. Since the S_1 state is dominantly described by the HOMO–LUMO single excitation, the shape of the involved orbitals helps to explain the geometry change. For instance, the π-orbitals located in the acetylenic bond change from bonding to antibonding character upon electronic excitation; the bond thus concomitantly elongates. On the other hand, the optimized geometry for the first triplet excited state remains almost unaltered at the end rings. In fact, considering a cutoff of |0.05 Å|, the geometric deformation taking place in the triplet state indicates how the exciton is more confined[65] and mainly localized at the acetylenic groups and central benzene ring.

3.2 Transition energies

Before commenting the results of the calculations we shall discuss first how to obtain and to compare experimental and theoretical results since gas-phase spectra are not available and thus the comparison with experiment is not straightforward. The photoluminescence data were recorded at 300 K from a spin-coated thin film of the organic molecule studied.[66] The experimental energy was thus taken from the position of the lowest vibronic feature (F_1) of the emission spectrum of the molecule; which is believed to be a reasonable first approximation to the optical band-gap (defined here as the adiabatic transition energy 0–0). The absence of the corresponding absorption (or low-temperature emission) spectra precludes to estimate the band-gap by other methods (onset of the

 This journal is © the Owner Societies 2008

View Article Online

Published on 06 March 2008. Downloaded by Michigan State University on 23/01/2016 03:07:12.

absorption spectra, intersection of the emission and absorption spectra or convolution of the resolved features observed in the low-temperature emission spectra).[13] The 0–0 energy for a broad set of conjugated molecules is located about 30 meV above the highest fluorescence sub-band F_1,[13] which thus confirm the procedure followed here. Furthermore, since theoretical calculations on isolated molecules correspond to gas-phase data at 0 K, the comparison with the experimental results would thus require explicit consideration of solid-state matrix effects. Despite the large variety of spectral changes observed experimentally for unsubstituted π-conjugated molecules, we consider a crystal shift of the order of 0.3 ± 0.1 eV reasonably close to what would be expected for this case.[13] The corresponding singlet–triplet transition energies were actually inferred from the experimental singlet–singlet value according to the procedure described in ref. 17. The singlet–triplet splitting (Δ_{ST}), which is also known as exchange energy, is simply the energy difference between these 0–0 transitions. The experimental vertical transition energy associated with the lowest absorption band was derived by adding to the 0–0 experimental energy the reorganization energy in the lowest excited state.[67] We have considered a value of 0.2 ± 0.1 eV from the results of increasingly longer rigid-rod oligophenylenevinylenes.[67,68] Note that we neglect at this stage zero-point energy differences between ground and excited states. A good estimate for the accuracy of the experimentally derived values might be of the order of ± 0.3 eV. Table 2 lists the experimental transition energies obtained with this procedure.

The transition energies calculated by the CASSCF method using all the selected active spaces are also gathered in Table 2. Note that the largest active space used, which leads to about 2×10^5 spin-adapted configuration state functions (CSF) for the molecule considered here, is of the same size than those used in previous studies of conjugated systems such as all-trans linear oligoenes,[69,70] short oligothiophenes[71,72] and porphyrins.[73] The electronic character of the ground and excited states as given by the coefficients of the main CSFs which absolute value is greater than 0.1 is listed in Table 3. A way to simplify the interpretation of the CASSCF wavefunction is to use the concept of natural orbital occupation numbers (NOON), which sum to the total number of electrons in the active space. The NOON values serve as indicators of the multireference character, ranging from 0 to 2 for a closed-shell, although a state with unpaired electrons will have some NOON close to 1. A marked deviation from these limiting values thus indicates significant multireference character. The NOON values for the S_0, S_1, and T_1 corresponding to the CASSCF(12,12) wavefunction are given in Fig. 3. Following the usual nomenclature, natural orbitals are labeled HOMO (H), (H-1)OMO, LUMO (L), (L + 1)UMO, and so on. The data shown in Table 3 indicate that the first singlet excited state comprises a considerable larger participation of a manifold of excitations than both the ground or the first triplet excited states. The models based on single electron transitions (configuration interaction singles or related methods as INDO/SCI) oversimplify somehow the nature of the excitations.[32]

We examine first the convergence of the results upon systematic increase of the active space, as already explained in section 2. Fig. 4 shows the variation of the relative energies ($E_{S_1} - E_{S_0}$ and $E_{T_1} - E_{S_0}$) and how a reasonable convergence with respect to the size of the active space (within ± 0.1 eV) is achieved at the (12,12) level for both adiabatic transitions. By comparing next the CASSCF results from Table 2 and Fig. 4 with those from the MRMP2 correction one can disentangle the effects associated with both types of electronic correlation since dynamic correlation contributions to the excitation energies are obtained from the CASSCF wavefunction through the perturbation treatment. By inspecting again the data compiled in Table 2, the most accurate CASSCF(12,12)-MRMP2 excitation energies are found to be overestimated by less than 0.3 eV with respect to the experimental results; which can be considered within the typical error of the method (0.1–0.3 eV).[74–76] We should stress that the overall accuracy of the results for the transition energies is high, even for the

Table 2 Total energies (in hartrees) for the ground and low-lying states of the phenylene ethylene oligomer using several methods. The corresponding transition energies (in eV) and their energy difference (Δ_{ST}) are also included. All quantities are calculated with the cc-pVDZ basis sets

Method	E_{S_0}	E_{T_1}	E_{S_1}	$E_{T_1} - E_{S_0}$	$E_{S_1} - E_{S_0}$	Δ_{ST}
CASSCF(2,2)	−1069.0297832[a]	−1068.8942770[a]	−1068.8226367[a]	3.69[a]	5.64[a]	1.95
		−1068.9172415[b]	−1068.8372336[b]	3.06[b]	5.24[b]	2.18
CASSCF(4,4)	−1069.0463244[a]	−1068.9238506[b]	−1068.8461934[b]	3.33[b]	5.45[b]	2.12
CASSCF(12,12)	−1069.1360929[a]	−1069.0070092[b]	−1068.9279618[b]	3.51[b]	5.66[b]	2.15
CASSCF(2,2)-MRMP2	−1072.5115138[a]	−1072.3920535[a]	−1072.3756654[a]	3.25[a]	3.70[a]	0.45
		−1072.4112586[b]	−1072.3965556[b]	2.73[b]	3.13[b]	0.40
CASSCF(4,4)-MRMP2	−1072.5137118[a]	−1072.4218416[b]	−1072.4043704[b]	2.50[b]	2.98[b]	0.48
CASSCF(12,12)-MRMP2	−1072.5666929[a]	−1072.4731732[b]	−1072.4463422[b]	2.54[b]	3.28[b]	0.73
BLYP	−1075.3517364[c]	−1075.2815210[c]	—	1.91[c]	—	—
BLYP (TD-DFT)				2.02	3.07	1.05
B3LYP	−1075.7857470[c]	−1075.7056735[c]	—	2.18[c]	—	—
B3LYP (TD-DFT)				2.20	3.28	1.08
Experimental (adiabatic)[d]				2.2	3.2	1.0
Experimental (vertical)[e]				2.4	3.4	1.0

[a] Energies evaluated at the CASSCF optimized geometry of the S_0 state. [b] Energies evaluated at the CASSCF optimized geometry of the corresponding state. [c] Energies evaluated at the DFT optimized geometry of the corresponding state. [d] Taken from ref. 66 and corrected with the crystal shift. [e] Taken from ref. 66 and corrected with both the crystal shift and reorganization energy.

View Article Online

Published on 06 March 2008. Downloaded by Michigan State University on 23/01/2016 03:07:12.

Table 3 Coefficients and occupancy (ignoring core) of the main CSFs entering into the CASSCF(12,12) wavefunction for each state

State	Coefficient (occupancy)		
^1A_g	0.907159 (222222000000)	−0.117666 (222022020000)	
^1B_u	0.750745 (222221100000)	−0.395455 (222122100000)	0.219287 (222221000100)
	−0.185458 (222122000100)	0.134368 (222212010000)	−0.121786 (222122000001)
	0.120098 (222221000001)		
^3B_u	0.901956 (222221100000)	−0.126265 (222122100000)	−0.122319 (222111111000)
	−0.110705 (112221100011)		

smallest active space, when the MRMP2 correction is added. We can thus infer that the dynamic electron correlation effects are essential for the highest accuracy of the excitation energies. As can be easily observed, the ultimate quality of the results crucially depends on the choice and size of the active space. However, the singlet–triplet splitting is a quite sensitive property since a well-balanced treatment of both states is a must. Quantitative results for the singlet–triplet splitting could only be obtained when the correlation treatment encompasses the largest (π-electrons, π-orbitals) space and the corresponding perturbation correction starting from that wavefunction. These are very time-consuming calculations requiring about 16 GB of memory, which are possible to run thanks to the capability of the code in GAMESS to partition large arrays across the memory of multiple nodes.[77] Note that one of the major advances of the code is the scalability of the methods for correlated calculations with respect to the number of cores used.[78] On the other hand, pure DFT (BLYP) and DFT-hybrid (B3LYP) do not lead to very similar excitation energies, as expected.[17] Note that the results provided by one or other functional might vary up to (0.2–0.3) eV with B3LYP the closest to the experimental values. Notwithstanding this, the TD-DFT B3LYP calculations give values for the excitation energies which are as reliable as the CASSCF(12,12)-MRMP2 adiabatic ones for this system, giving strong support to the procedure described above to deduce the transition energies from the available experimental data within the estimated error bars. Unfortunately, the good performance of the B3LYP exchange–correlation functional to reproduce the excitation energies of this molecule is not matched for the torsional barrier, as shown below.

3.3 Rotational barrier

Turning now to the discussion mentioned in the Introduction about the rotational barrier height, the relative energies for the optimized geometries of the ground state at each twisting angle (0 and 90°) are presented in Table 4. We note the well-known fact that complete rotation of the middle ring with respect to the side moieties, that is, around the trans-annular CC bonds, decreases the overlap between the phenyl π-electron cloud and one of the π-bond of each acetylenic bond; and hence the delocalization of the π-electron density. However, at the fully twisted geometry the second (in-plane) π-bond of each acetylenic bond may partially compensate that loss of π-delocalization. The interplay between these two situations causes a rather flat potential energy surface which translates into a very small value for the experimental barrier height (28.3 ± 0.2 meV as measured using the highly sensitive cavity ring-down spectroscopy, for details see ref. 40). Since the rotational barrier is below 1 kcal/mol, such a tiny energy difference thus represents a challenge for any theoretical method. The analysis of the *ab initio* results with the cc-pVDZ basis sets allows us to conclude that: (i) a compensation of errors leads to a HF result fortuitously close to the experimental value (see below); (ii) the small active space for the CASSCF wavefunction is not enough to reach accurate predictions and will thus not be shown; (iii) when the active space is made as complete as possible, the non-dynamic correlation helps to improve the barrier height; and (iv) the inclusion of a large portion of the dynamic correlation at the MRMP2 level seems to deteriorate the results due to a non-balanced treatment of the planar and highly twisted geometries, which has been previously

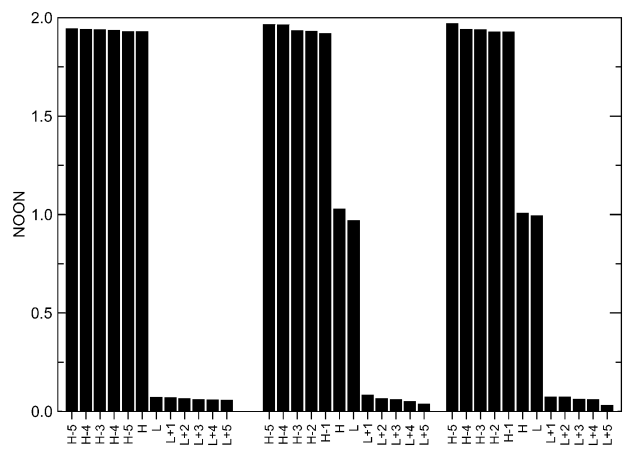

Fig. 3 Natural orbital occupation numbers for the ground and first excited singlet and triplet states (from left to right).

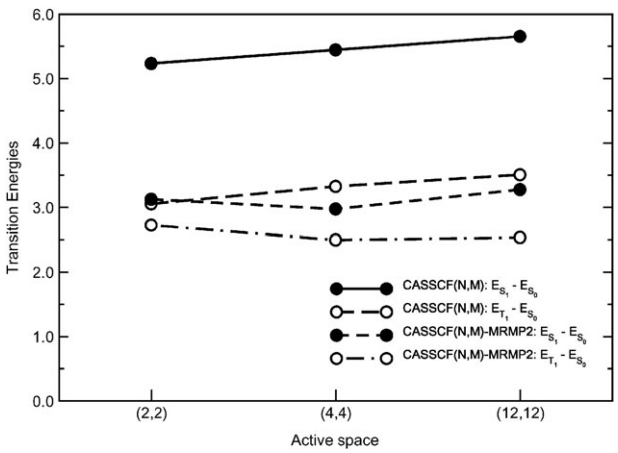

Fig. 4 Convergence of the lowest singlet and triplet transition energies (in eV) as a function of an increasingly large active space.

 This journal is © the Owner Societies 2008

View Article Online

Published on 06 March 2008. Downloaded by Michigan State University on 23/01/2016 03:07:12.

Table 4 Torsional barrier height (in meV) for the rotation of the central ring of the phenylene ethylene oligomer using several methods and basis sets. The SEC acronym refers to the scaled external correlation method, see text for details

Method	$E(90^\circ) - E(0^\circ)$
RHF/cc-pVDZ	39.2
RHF/cc-pVTZ	41.8
RHF/cc-pV∞Z	42.6
CASSCF(12,12)/cc-pVDZ	23.6
CASSCF(12,12)-MRMP2/cc-pVDZ	47.5
CASSCF(12,12)-MRMP2/cc-pV∞Z	49.6
SEC-CASSCF(12,12)-MRMP2/cc-pVDZ	35.7
SEC-CASSCF(12,12)-MRMP2/cc-pV∞Z	37.7
SEC-CASSCF(12,12)-MRMP2/cc-pV∞Z + ZPVE	33.2
BLYP/cc-pVDZ	118.0
BLYP/cc-pVDZ + ZPVE	113.5
B3LYP/cc-pVDZ	97.1
B3LYP/cc-pVDZ + ZPVE	92.6
Experimental[a]	28.3 ± 0.2

[a] Taken from ref. 40.

documented.[79] The inclusion of the MP2-based dynamic correlation energy deteriorates the rotational barrier independently of the use of a mono- or a multi-configurational wavefunction. In fact, we have performed additional MP2/cc-pVDZ calculations to obtain a value of 68.8 meV for the barrier height. Our experience concerning calculated torsional barrier heights tells us that at least extending the perturbation series up to fourth order (MP4) is necessary to obtain more accurate values.[80–83] However, it will be shown below that when several correcting terms are taken into account the results achieve a much better agreement with the experimental data.

We first proceed to analyze the influence of augmenting the size of the basis sets on the results. However, incrementing the basis set size while keeping the large active spaces needed for quantitative purposes goes beyond our present computational capabilities. Accordingly, we will exploit the systematic convergence of the cc-pVnZ basis sets. The infinite basis set limit (cc-pV∞Z) may be estimated by using well-defined extrapolation techniques.[84,85] For the HF energy, we use the function:[86]

$$E_{\mathrm{HF}}(n) = E_{\mathrm{HF}}(\infty) + An^{-3.39}, \quad (1)$$

where $E_{\mathrm{HF}}(\infty)$ is the corresponding extrapolated energy and A is the parameter to be fitted by employing the results from two basis sets (cc-pVDZ and cc-pVTZ). Regardless of the active space used, the non-dynamic correlation energy is virtually independent of the basis sets[87] and will thus not be extrapolated. The fraction of the dynamic correlation energy lost is roughly recovered by the use of the model:[88]

$$E_c(n) = E_c(\infty)\{1 - 2.4n^{-3}[1 + (ae^{-2.4b} + c)n^{-1}]\}, \quad (2)$$

where a, b, and c are a set of optimal parameters for fitting the input data sets as extracted from the original work.[88] The corresponding extrapolated results are also reported in Table 4. It can be concluded that the barrier height does not largely depend on the basis sets at the correlated level.

We discuss next an additional correction to approach the near-exact result based on a balanced treatment of the dynamical correlation energy for both the planar and twisted geometries. Thus, following Truhlar *et al.*[89] we use the so-called "scaled external correlation" (SEC) method and apply a scaling factor to the dynamic correlation energy. The justification is that for a given level of treating electron correlation and a given basis set, the fraction of the dynamic correlation energy which is still missed may be recovered if scaled by a factor larger than unity. The final energy for the one-electron basis sets under consideration (cc-pVDZ or extrapolated cc-pV∞Z) is thus approximated as:

$$E_{\mathrm{SEC}} = E_{\mathrm{CASSCF(12,12)}} + \frac{E_{\mathrm{CASSCF(12,12)-MRMP2}} - E_{\mathrm{CASSCF(12,12)}}}{F}. \quad (3)$$

The parameter F may be determined either from accurate *ab initio* calculations or from available experimental results.[90,91] Note that we do not assume that F is independent of the geometry. In fact, we calculate this parameter for the planar (0°) and completely twisted (90°) geometries by resorting to a molecule (styrene) for which the torsional profile[92] closely resembles the one calculated for this molecule;[17] which indeed indicates the existence of the same kind of stereo-electronic effects. The value of F is then calculated using the expression:

$$F = \frac{E_{\mathrm{MP2}} - E_{\mathrm{HF}}}{E_{\mathrm{CCSD(T)}} - E_{\mathrm{HF}}}, \quad (4)$$

where E_{MP2} and $E_{\mathrm{CCSD(T)}}$ are, respectively, the Møller–Plesset perturbative expansion up to second order and the coupled-cluster singles, doubles and perturbatively estimated triplet energies. Note that we also assume the same convergence pattern for the calculated single- and multi-configurational dynamic correlation. This procedure have yielded values of $F_{0^\circ} = 0.91036$ and $F_{90^\circ} = 0.91023$; which significantly improves the barrier height as can be easily verified from Table 4. The small difference found between F_{0° and F_{90° merely corroborates that the fraction of the correlation energy is more a function of the theoretical level than of the geometry.

It is easy now to understand why the barrier height predicted at the uncorrelated HF level is fortuitously close to the most accurate value. We first define the following increments (in meV) to be added to the RHF/cc-pVDZ calculated value:

$$\Delta E_c^{\text{non-dynamic}} = E_{\mathrm{CASSCF(12,12)/cc\text{-}pVDZ}} - E_{\mathrm{RHF/cc\text{-}pVDZ}} = -15.6, \quad (5)$$

$$\Delta E_c^{\text{dynamic}} = E_{\mathrm{CASSCF(12,12)\text{-}MRMP2/cc\text{-}pVDZ}} - E_{\mathrm{CASSCF(12,12)/cc\text{-}pVDZ}} = 23.9 \quad (6)$$

$$\Delta E_c^{\text{dynamic}'} = E_{\mathrm{SEC\text{-}CASSCF(12,12)\text{-}MRMP2/cc\text{-}pVDZ}} - E_{\mathrm{CASSCF(12,12)\text{-}MRMP2/cc\text{-}pVDZ}} = -11.8 \quad (7)$$

$$\Delta E_c^{\text{dynamic}''} = E_{\mathrm{SEC\text{-}CASSCF(12,12)\text{-}MRMP2/cc\text{-}pV\infty Z}} - E_{\mathrm{SEC\text{-}CASSCF(12,12)\text{-}MRMP2/cc\text{-}pVDZ}} = 2.0, \quad (8)$$

which leads to the following final result (in meV) for the correlation contributions to the uncorrelated value:

$$\Delta E_c = \Delta E_c^{\text{non-dynamic}} + (\Delta E_c^{\text{dynamic}} + \Delta E_c^{\text{dynamic}'} + \Delta E_c^{\text{dynamic}''}) = -1.5. \quad (9)$$

The barrier height remains almost unaltered after adding the correlation energy, which thus clearly attributes the accurate HF value to a compensation of errors.

View Article Online

Published on 06 March 2008. Downloaded by Michigan State University on 23/01/2016 03:07:12.

Finally, we have considered the differences in the zero-point vibrational energies (ZPVEs) of the two conformations. First, the harmonic vibrational frequencies are calculated at the B3LYP/cc-pVDZ level, which also truly confirm the planar (highly twisted) form as the global minimum (transition state). Next, low frequencies modes are subtracted out from the ZPVEs since translation and rotational contributions need to be eliminated. The final ZPVE-corrected value for the barrier (33.2 meV) is in very good agreement with the experimental result (28.3 ± 0.2 meV). Note that for the very highest accuracy, which is beyond the goal of the study, other minor effects such as core-valence correlation[80] or relativistic effects[81] might be also included.

On the other hand, the torsional barrier height is largely overestimated by the DFT calculations, probably due to the inability of current exchange functionals to describe π-bond breaking effects experienced by conjugated molecules,[93–96] with B3LYP methods being slightly more accurate than BLYP. The type of correlation functional itself makes little difference.[17] The overestimation warns about quantitative studies of reversible processes based on the rotation of the central moiety of conjugated molecules using KS DFT calculations. A careful and systematic study in nanoscale investigations is thus always recommended when DFT is chosen in view of its reduced computational cost.

4. Concluding remarks

In summary, we have sought to demonstrate how multi-configurational theories are a good starting point for accurate calculations on conjugated molecular systems of chemical interest close to the experimental accuracy. Even though these calculations in practice require much more technicalities than approximate methods of somehow 'black-box' usage, semi-empirical or DFT-based, they are known to lead, however, to quantitative results for ground-state properties and excitation energies of both planar and twisted forms. Furthermore, whereas the results from an *ab initio* method can be scaled or extrapolated to approximate higher orders of the hierarchy, the same systematic improvement may not be easily found for the latter. Since an *a priori* decision on the structure of the wavefunction needs to be done, which is additionally limited by the high computational requirements of the algorithms, we have provided an example of the kind of calculation that could be performed with present day large-memory multi-core computers. Note that for increasingly larger conjugated organic molecules, the active space would probably need to be severely truncated, which could deteriorate the accuracy of the results. On the other hand, when chain lengths get longer, DFT is known to be affected by cumulative and size-extensive errors[97–101] which may become larger than the previous one.[102] Therefore, with all due caution that should be taken when computational methods are applied to charge-transfer or optical processes for conjugated organic molecules, further care must be recommended when using more approximated (less systematic) methods.

Acknowledgements

This work is supported by the "Ministerio de Educación y Ciencia" of Spain and the "European Regional Development Fund" through projects CTQ2004-06519/BQU and CTQ2007-66461/BQU; the regular grants of the "Vicerrectorado de Investigación" of the University of Alicante (VIGROB2005-96) are also acknowledged. The two authors also thank the "Ministerio de Educación y Ciencia" of Spain for a research contract under the "Ramón y Cajal" program, and to the "Generalitat Valenciana" for further economic support.

References

1 J.-L. Brédas, D. Beljonne, V. Coropceanu and J. Cornil, *Chem. Rev.*, 2004, **104**, 4971.
2 P. Hohenberg and W. Kohn, *Phys. Rev. B*, 1964, **136**, 864.
3 W. Kohn and L. J. Sham, *Phys. Rev. A*, 1965, **140**, 1133.
4 W. Koch and M. Holthausen, *A Chemist's Guide to Density Functional Theory*, Wiley-VCH, Weinheim, 2001.
5 J. Reimers, Z.-L. Cai, A. Bilić and N. S. Hush, *Ann. N. Y. Acad. Sci.*, 2003, **1006**, 235.
6 N. T. Maitra, K. Burke, H. Appel, E. K. U. Gross and R. van Leeuwen, in *Reviews of Modern Quantum Chemistry*, ed. K. D. Sen, World Scientific, Singapore, 2002.
7 F. Furche and K. Burke, *Ann. Rep. Comp. Chem.*, 2005, **1**, 19.
8 K. Burke, J. Werschnik and E. K. U. Gross, *J. Chem. Phys.*, 2005, **123**, 062206.
9 U. Salzner, P. G. Pickup, R. A. Poirier and J. B. Lagowski, *J. Phys. Chem. A*, 1998, **102**, 2572.
10 U. Salzner, *Curr. Org. Chem.*, 2004, **8**, 569.
11 M. Dierksen and S. Grimme, *J. Phys. Chem. A*, 2004, **108**, 10225.
12 A. Dreuw and M. Head-Gordon, *Chem. Rev.*, 2005, **105**, 4009.
13 J. Gierschner, J. Cornil and H.-J. Egelhaaf, *Adv. Mater.*, 2007, **19**, 1.
14 R. J. Magyar and S. Tretiak, *J. Chem. Theory Comput.*, 2007, **3**, 976.
15 U. Salzner, *J. Chem. Theory Comput.*, 2007, **3**, 1143.
16 J. C. Sancho-García, *Chem. Phys.*, 2007, **331**, 321.
17 J. C. Sancho-García, *Chem. Phys. Lett.*, 2007, **439**, 236.
18 A. Pogantsch, G. Heimel and E. Zojer, *J. Chem. Phys.*, 2002, **117**, 5921.
19 S. Grimme and M. Parac, *ChemPhysChem.*, 2003, **3**, 292.
20 P. Marsal, I. Avilov, D. A. da Silva, J. L. Brédas and D. Beljonne, *Chem. Phys. Lett.*, 2004, **392**, 521.
21 M. Wanko, M. Garavelli, F. Bernardi, T. A. Niehaus, T. Frauenheim and M. Elstner, *J. Chem. Phys.*, 2004, **120**, 1674.
22 D. Jacquemin, E. A. Perpète, I. Ciofini and C. Adamo, *Chem. Phys. Lett.*, 2005, **405**, 376.
23 E. Fabiano, F. Della Sala, R. Cingolani, M. Weimer and A. Görling, *J. Phys. Chem. A*, 2005, **109**, 3078.
24 D. Wasserberg, P. Marsal, S. C. J. Meskers, R. A. J. Janssen and D. Beljonne, *J. Phys. Chem. B*, 2005, **109**, 4410.
25 M. Weimer, W. Hieringer, F. Della Sala and A. Görling, *Chem. Phys.*, 2005, **309**, 77.
26 R. S. Sánchez-Carrera, V. Coropceanu, D. A. da Silva Filho, R. Friedlein, W. Osikowicz, R. Murdey, C. Suess, W. R. Salaneck and J. L. Brédas, *J. Phys. Chem. B*, 2006, **110**, 18904.
27 T. Grabo, T. Kreibich, S. Kurth and E. K. U. Gross, in *Strong Coulomb correlations in electronic structure: beyond the local density approximation*, ed. V. I. Anisimov, Gordon and Breach, Tokyo, 1998.
28 F. Della Sala and A. Görling, *J. Chem. Phys.*, 2001, **115**, 5718.
29 A. Görling, *J. Chem. Phys.*, 2005, **123**, 062203.
30 S. Grimme, *J. Chem. Phys.*, 2006, **124**, 034108.
31 R. J. Cave, in *Modern Electronic Structure Theory and Applications in Organic Chemistry*, ed. E. R. Davidson, World Scientific, Singapore, 1997.
32 L. Serrano-Andrés and M. Merchán, *THEOCHEM*, 2005, **729**, 99.
33 M. van Faassen, P. L. de Boeij, R. van Leeuwen, J. A. Berger and J. G. Snijders, *Phys. Rev. Lett.*, 2002, **88**, 186401.
34 A. Aviram and M. A. Ratner, *Chem. Phys. Lett.*, 1974, **29**, 277.
35 M. A. Reed, C. Zhou, C. J. Muller, T. P. Burgin and J. M. Tour, *Science*, 1997, **278**, 252.

 This journal is © the Owner Societies 2008

View Article Online

Published on 06 March 2008. Downloaded by Michigan State University on 23/01/2016 03:07:12.

36 J. M. Tour, *Molecular Electronics*, World Scientific, Singapore, 2003.
37 V. Balzani, A. Credi and M. Venturi, *Molecular Devices and Machines*, Wiley-VCH, Weinheim, 2004.
38 F. Jiang, Y. X. Zhou, H. Chen, R. Note, H. Mizuseki and Y. Kawazoe, *Phys. Lett. A*, 2006, **359**, 487.
39 S. Yeganeh, M. Galperin and M. Ratner, *J. Am. Chem. Soc.*, 2007, **129**, 13313.
40 S. J. Greaves, E. L. Flynn, E. L. Futcher, E. Wrede, D. P. Lydon, P. J. Low, S. R. Rutter and A. Beeby, *J. Phys. Chem. A*, 2006, **110**, 2114.
41 M. Levitus, K. Schmieder, H. Ricks, K. D. Shimizu, U. H. F. Bunz and M. A. García-Garibay, *J. Am. Chem. Soc.*, 2001, **123**, 4259.
42 R. J. Magyar, S. Tretiak, Y. Gao, H.-L. Wang and A. P. Shreve, *Chem. Phys. Lett.*, 2005, **401**, 149.
43 P. V. James, P. K. Sudeep, C. H. Suresh and K. G. Thomas, *J. Phys. Chem. A*, 2006, **110**, 4329.
44 L. Serrano-Andrés, M. Merchán and M. Jabloński, *J. Chem. Phys.*, 2003, **119**, 4294.
45 Y. Amatatsu and Y. Hasebe, *J. Phys. Chem. A*, 2003, **107**, 11169.
46 I. Pugliesi, N. M. Tonge, K. E. Hornsby, M. C. R. Cockett and M. J. Watkins, *Phys. Chem. Chem. Phys.*, 2007, **9**, 5436.
47 Y. Amatatsu and M. Hosokawa, *J. Phys. Chem. A*, 2004, **108**, 10238.
48 M. W. Schmidt and M. S. Gordon, *Annu. Rev. Phys. Chem.*, 1998, **49**, 233.
49 H. Nakano, *J. Chem. Phys.*, 1993, **99**, 7983.
50 H. Nakano, *Chem. Phys. Lett.*, 1993, **207**, 372.
51 M. W. Schmidt, K. K. Baldridge, J. A. Boatz, S. T. Elbert, M. S. Gordon, J. H. Jensen, S. Koseki, N. Matsunaga, K. A. Nguyen, S. J. Su, T. L. Windus, M. Dupuis and J. A. Montgomery, *J. Comput. Chem.*, 1993, **14**, 1347.
52 E. R. Davidson and A. A. Jarzecki, in *Recent Advances in Multi-reference Methods*, ed. K. Hirao, WorldScientific, Singapore, 1999.
53 D. K. W. Mok, R. Neumann and N. C. Handy, *J. Phys. Chem.*, 1996, **100**, 6225.
54 S. Grimme and M. Waletzke, *Phys. Chem. Chem. Phys.*, 2000, **2**, 2075.
55 J. M. Rintelman, I. Adamovic, S. Varganov and M. S. Gordon, *J. Chem. Phys.*, 2005, **122**, 044105.
56 D. Robinson and J. W. McDouall, *J. Chem. Theory Comput.*, 2007, **3**, 1306.
57 B. O. Ross, M. Fülscher, P.-Å. Malmqvist, M. Merchán and L. Serrano-Andrés, in *Quantum Mechanical Electronic Structure Calculations with Chemical Accuracy*, ed. S. R. Langhoff, Kluwer Academic Press, Dordrecht, 1995.
58 A. D. Becke, *Phys. Rev. A*, 1988, **38**, 3098.
59 C. Lee, W. Yang and R. G. Parr, *Phys. Rev. B*, 1988, **37**, 785.
60 A. D. Becke, *J. Chem. Phys.*, 1993, **98**, 5648.
61 P. J. Stephens, F. J. Devlin, C. F. Chablowski and M. J. Frisch, *J. Phys. Chem.*, 1994, **98**, 11623.
62 O. Gunnarsson and B. I. Lundqvist, *Phys. Rev. B*, 1976, **13**, 4274.
63 M. J. Frisch, G. W. Trucks, H. B. Schlegel, G. E. Scuseria, M. A. Robb, J. R. Cheeseman, J. A. Montgomery, Jr., T. Vreven, K. N. Kudin, J. C. Burant, J. M. Millam, S. S. Iyengar, J. Tomasi, V. Barone, B. Mennucci, M. Cossi, G. Scalmani, N. Rega, G. A. Petersson, H. Nakatsuji, M. Hada, M. Ehara, K. Toyota, R. Fukuda, J. Hasegawa, M. Ishida, T. Nakajima, Y. Honda, O. Kitao, H. Nakai, M. Klene, X. Li, J. E. Knox, H. P. Hratchian, J. B. Cross, V. Bakken, C. Adamo, J. Jaramillo, R. Gomperts, R. E. Stratmann, O. Yazyev, A. J. Austin, R. Cammi, C. Pomelli, J. Ochterski, P. Y. Ayala, K. Morokuma, G. A. Voth, P. Salvador, J. J. Dannenberg, V. G. Zakrzewski, S. Dapprich, A. D. Daniels, M. C. Strain, O. Farkas, D. K. Malick, A. D. Rabuck, K. Raghavachari, J. B. Foresman, J. V. Ortiz, Q. Cui, A. G. Baboul, S. Clifford, J. Cioslowski, B. B. Stefanov, G. Liu, A. Liashenko, P. Piskorz, I. Komaromi, R. L. Martin, D. J. Fox, T. Keith, M. A. Al-Laham, C. Y. Peng, A. Nanayakkara, M. Challacombe, P. M. W. Gill, B. G. Johnson, W. Chen, M. W. Wong, C. Gonzalez and J. A. Pople, *GAUSSIAN 03 (Revision C.02)*, Gaussian, Inc., Wallingford, CT, 2004.
64 B. N. Papas and H. F. Schaefer, III, *THEOCHEM*, 2006, **768**, 175.
65 D. Beljonne, J. Cornil, R. H. Friend, R. A. J. Janssen and J.-L. Brédas, *J. Am. Chem. Soc.*, 1996, **118**, 6453.
66 A. Köhler, J. S. Wilson, R. H. Friend, M. K. Al-Suti, M. S. Khan, A. Gerhard and H. Bässler, *J. Chem. Phys.*, 2002, **116**, 9457.
67 J. Gierschner, H.-G. Mack, L. Lüer and D. Oelkrug, *J. Chem. Phys.*, 2002, **116**, 8596.
68 J. C. Sancho-García, J. L. Brédas, D. Beljonne, J. Cornil, R. Martínez-Álvarez, M. Hanack, L. Poulsen, J. Gierschner, H.-G. Mack, H.-J. Egelhaaf and D. Oelkrug, *J. Phys. Chem. B*, 2005, **109**, 4872.
69 Y. Kurashige, H. Nakano, Y. Nakao and K. Hirao, *Chem. Phys. Lett.*, 2004, **400**, 425.
70 U. Salzner, *J. Chem. Theory Comput.*, 2007, **3**, 219.
71 M. Rubio, M. Merchán, R. Pou-Amérigo and E. Ortí, *ChemPhysChem.*, 2003, **4**, 1308.
72 M. Rubio, M. Merchán and E. Ortí, *Chem. Phys. Chem.*, 2005, **6**, 1357.
73 M. Radoń and E. Broclawik, *J. Chem. Theory Comput.*, 2007, **3**, 728.
74 M. Merchán, L. Serrano-Andrés, M. P. Fülscher and B. O. Roos, in *Recent Advances in Multi-reference Methods*, ed. K. Hirao, World Scientific, Singapore, 1999.
75 S. Grimme, M. Parac and M. Waletzke, *Chem. Phys. Lett.*, 2001, **334**, 99.
76 M. Parac and S. Grimme, *J. Phys. Chem. A*, 2002, **109**, 6844.
77 H. Umeda, S. Oseki, U. Nagashima and M. W. Schmidt, *J. Comp. Chem.*, 2001, **22**, 1243.
78 M. S. Gordon and M. W. Schmidt, in *Lectures Notes in Computer Science*, ed. P. M. A. Sloot *et al.*, Springer-Verlag, Berlin, 2003, vol. 2660.
79 K. Sakata and K. Hara, *Chem. Phys. Lett.*, 2003, **371**, 164.
80 J. C. Sancho-García and J. Cornil, *J. Chem. Theory Comput.*, 2005, **1**, 581.
81 A. J. Pérez-Jiménez, J. C. Sancho-García and J. M. Pérez-Jordá, *J. Chem. Phys.*, 2005, **123**, 134309.
82 J. C. Sancho-García and A. Karpfen, *Chem. Phys. Lett.*, 2005, **411**, 321.
83 J. C. Sancho-García and A. Karpfen, *Theor. Chem. Acc.*, 2006, **115**, 427.
84 D. W. Schwenke, *J. Chem. Phys.*, 2005, **122**, 014107.
85 A. J. C. Varandas, *J. Chem. Phys.*, 2007, **126**, 1953.
86 P. L. Fast, M. L. Sánchez and D. G. Truhlar, *J. Chem. Phys.*, 1999, **111**, 2921.
87 D. M. Smith, D. Barić and Z. B. Maksić, *J. Chem. Phys.*, 2001, **115**, 3474.
88 A. J. C. Varandas, *J. Chem. Phys.*, 2000, **113**, 8880.
89 F. B. Brown and D. G. Truhlar, *Chem. Phys. Lett.*, 1985, **117**, 307.
90 I. Rossi and D. G. Truhlar, *Chem. Phys. Lett.*, 1995, **234**, 64.
91 P. L. Fast, J. Corchado, M. L. Sánchez and D. G. Truhlar, *J. Phys. Chem. A*, 1999, **101**, 3139.
92 J. C. Sancho-García and A. J. Pérez-Jiménez, *J. Phys. B*, 2002, **35**, 1509.
93 J. C. Sancho-García, A. J. Pérez-Jiménez and F. Moscardó, *J. Phys. Chem. A*, 2001, **105**, 11541.
94 J. C. Sancho-García, J. L. Bredás and J. Cornil, *Chem. Phys. Lett.*, 2003, **377**, 63.
95 J. C. Sancho-García and J. Cornil, *J. Chem. Phys.*, 2004, **121**, 3096.
96 J. C. Sancho-García, *J. Chem. Phys.*, 2006, **124**, 124112.
97 M. D. Wodrich, C. Corminboeuf and P. von R. Schleyer, *Org. Lett.*, 2006, **8**, 3631.
98 P. R. Schreiner, A. A. Okin, R. A. Pascal and A. de Meijere, *Org. Lett.*, 2006, **8**, 3635.
99 Y. Zhao and D. G. Truhlar, *Org. Lett.*, 2006, **8**, 5753.
100 S. Grimme, *Angew. Chem. In. Ed.*, 2006, **45**, 4460.
101 S. Grimme, M. Steinmetz and M. Korth, *J. Org. Chem.*, 2007, **72**, 2118.
102 P. R. Schreiner, *Angew. Chem., Int. Ed.*, 2007, **46**, 4217.